THE BASTILLE DAY MAGNETIC CLOUDS AND UPSTREAM SHOCKS: NEAR-EARTH INTERPLANETARY OBSERVATIONS

R. P. LEPPING[1], D. B. BERDICHEVSKY[1,6], L. F. BURLAGA[1], A. J. LAZARUS[2], J. KASPER[2], M. D. DESCH[1], C.-C. WU[1,7], D. V. REAMES[1], H. J. SINGER[3], C. W. SMITH[4] and K. L. ACKERSON[5]

[1]*GSFC/NASA, Goddard Space Flight Center, Greenbelt, MD 20771, U.S.A.*
[2]*Center for Space Research; MIT; Cambridge, MA 02139, U.S.A.*
[3]*NOAA, Space Environment Center, Boulder, CO 80303, U.S.A.*
[4]*Bartol Research Institute, University of Delaware, Newark, Delaware 19716, U.S.A.*
[5]*Department of Physics and Astronomy, University of Iowa, IO 52242, U.S.A.*
[6]*Emergent Information Technology, Largo, MD 20774, U.S.A.*
[7]*NRC Research Fellow*

(Accepted 10 July 2001)

Abstract. The energetic charged particle, interplanetary magnetic field, and plasma characteristics of the 'Bastille Day' shock and ejecta/magnetic cloud events at 1 AU occurring over the days 14–16 July 2000 are described. Profiles of MeV (WIND/LEMT) energetic ions help to organize the overall sequence of events from the solar source to 1 AU. Stressed are analyses of an outstanding magnetic cloud (MC2) starting late on 15 July and its upstream shock about 4 hours earlier in WIND magnetic field and plasma data. Also analyzed is a less certain, but likely, magnetic cloud (MC1) occurring early on 15 July; this was separated from MC2 by its upstream shock and many heliospheric current sheet (HCS) crossings. Other HCS crossings occurred throughout the 3-day period. Overall this dramatic series of interplanetary events caused a large multi-phase magnetic storm with min *Dst* lower than -300 nT. The very fast solar wind speed (≥ 1100 km s^{-1}) in and around the front of MC2 (for near average densities) was responsible for a very high solar wind ram pressure driving in the front of the magnetosphere to geocentric distances estimated to be as low as $\approx 5\ R_E$, much lower than the geosynchronous orbit radius. This was consistent with magnetic field observations from two GOES satellites which indicated they were in the magnetosheath for extended times. A static force-free field model is used to fit the two magnetic cloud profiles providing estimates of the clouds' physical and geometrical properties. MC2 was much larger than MC1, but their axes were nearly antiparallel, and their magnetic fields had the same left-handed helicity. MC2's axis and its upstream shock normal were very close to being perpendicular to each other, as might be expected if the cloud were driving the shock at the time of observation. The estimated axial magnetic flux carried by MC2 was 52×10^{20} Mx, which is about 5 times the typical magnetic flux estimated for other magnetic clouds in the WIND data over its first 4 years and is 17 times the flux of MC1. This large flux is due to both the strong axially-directed field of MC2 (46.8 nT on the axis) and the large radius ($R_0 = 0.189$ AU) of the flux tube. MC2's average speed is consistent with the expected transit time from a halo-CME to which it is apparently related.

Solar Physics **204:** 287–305, 2001.

1. Introduction

We describe here the solar wind, magnetic field and energetic particle observations at 1 AU of the Bastille Day ejecta/magnetic cloud complex of events stressing the roles and analyses of the magnetic clouds and their upstream shocks. For our purposes the region of interest extends over almost three days in mid-July 2000, starting on the 14th (Day of year = 196). We present, first, descriptions and analyses of two magnetic clouds (occurring on 15 and 16 July), second, analysis of a shock (S2) observed about 4 hours upstream of the boundary of the 2nd cloud (MC2) and which was apparently driven by that cloud, and third, a description of an even earlier interplanetary shock (S1) upstream of the 1st magnetic cloud (MC1). The interplanetary and solar aspects of these events were measured by an unprecedented number of instruments in interplanetary space, including (at least) those on SOHO, WIND, GEOTAIL, NEAR, ACE, and IMP-8; see Smith *et al.* (2001) for a comprehensive overview of the ACE interplanetary observations. From SOHO/EIT LASCO observations we gain information on the solar source of these events, and from the other spacecraft we obtain data allowing the analysis of MC2's upstream shock, S2, but we concentrate primarily on WIND data [from MFI (Lepping *et al.*, 1995) and SWE (Ogilvie *et al.*, 1995)] to analyze the two magnetic clouds. (MC2 was seen in NEAR spacecraft data also and its ACE and NEAR observations were compared with good agreements (Mulligan *et al.*, 2001); NEAR was 1.76 AU from the Sun and fortuitously close to conjunction with Earth.) It is seen that time profiles of MeV energetic ions made by the WIND/LEMT (von Rosenvinge *et al.*, 1995) help to organize the sequence of physical events comprising the Bastille Day complex of events, from the source, at about 30 to 60 min after the solar lift-off of the ejected material (in which supposedly strong helical field-lines systems are imbedded) to the time of the two shock-cloud passages at Earth.

The strong shock S2 was observed at WIND at 14:35 UT, on 15 July 2000, followed by the apparent shock-driver, the large interplanetary magnetic cloud itself, starting shortly thereafter. Although MC2 lasted only about 15 hours from start to finish, because of its unusually large average speed of about 1000 km s^{-1} at 1 AU, it was estimated to have a radius among the largest ever observed at 1 AU. For comparison, the average central speeds of 34 magnetic clouds occurring during the first 4 years of WIND data was only 400 ($\pm$ 50) km s^{-1} (Lepping and Berdichevsky, 2000).

Figure 1 shows the energetic particle flux (1st, or top panel), magnetic field and plasma profiles of the overall shocks-clouds complex. The magnetic field is given in panels 2–4 and plasma in panels 5–7. Table I gives an ordered outline of significant events from the solar source, upstream ambient solar wind to the plasma after MC2 passage. The earlier interplanetary shock (called S1) at 15:29 UT on 14 July, as well as the stream conditions observed afterward in the interplanetary medium, can be related to an earlier halo-CME observed at 13:27 UT on 11 July. When magnetic clouds are observed at 1 AU they are often associated with the

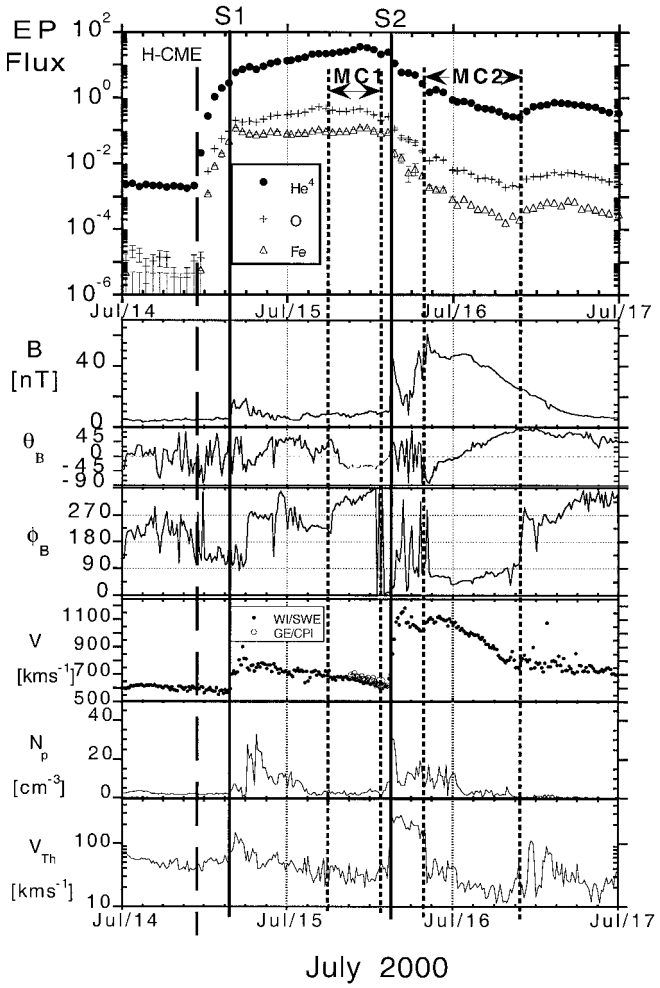

Figure 1. A three-day overview of the complex of events in terms of (*from top to bottom*): the energetic particle flux (in units of [cm^2 sr s MeV]$^{-1}$ from WIND/LEMT), magnetic field (magnitude, |**B**|; latitude, θ_B; and longitude, ϕ_B, respectively, from WIND/MFI), and plasma quantities (bulk speed, V; proton density, N_P; and proton thermal speed, $V_{\rm Th}$). (All are in 15 min average form.) The three species of energetic particles are shown by the key where a *filled dot* represents 7.4–9.64 MeV nucl^{-1} (n) of He^4, a *cross* is 9.2–13.4 MeV nucl^{-1} of O, and a *triangle* is 9.3–12.5 MeV nucl^{-1} of Fe. When θ_B is negative the region between the curve and the zero line is shaded, to alert the reader of likely regions of solar wind-magnetosphere coupling. H-CME (*big dashed vertical line*) indicates the time of a halo coronal mass ejection, S1 and S2 (*solid vertical lines*) designate interplanetary shocks, MC2 indicates a magnetic cloud, and MC1 is a likely magnetic cloud (see text); the boundaries of these clouds are indicated by *dashed lines*. The speeds (as are all plasma quantities) are from WIND/SWE investigation, except for those in region of about 8 hours just before S2, which are from GEOTAIL/CPI and shown by open circles.

TABLE I
Schedule of events during the shock/ejecta/magnetic cloud complex.

Event	Start time[a]		End time		Comments
	day[b]	UT[c]	day[b]	UT[c]	
Solar source	14	11			As seen by energetic particles[d].
1st IP shock (S1)	14	15:29			Apparently a pulsation shock. It lacks a sharp ramp in $\|\mathbf{B}\|$. SSC occurred at 15:32 UT.
Magnetic cloud (MC1) in Ejecta complex	15	06	15	14	The identity as a MC suffers some uncertainty, because of its IMF profile and small size.
2nd IP shock (S2)	15	14:35			Shock driven by the following MC. SSC occurred at 14:37 UT.
Magnetic cloud (MC2)	15	19	16	09	Very fast moving MC with very strong magnetic (B_s) field.
Post-cloud ejecta	16	09	?		

[a]In the case of a shock or discontinuity only a single time (start) is given, because start and end are indistinguishable on the scale considered here.
[b]Day refers to day of July 2000.
[c]UT refers to hour and minute resolution, unless time is resolved to 1-hour as it is for the magnetic clouds ejecta.
[d]From WIND/LEMT observations.

occurrence of halo-CMEs about 3 days earlier (e.g., Gopalswamy *et al.*, 1998; Webb *et al.*, 2000); also see Gosling (1990). The disturbed conditions observed many hours after the passage of S1 may correspond to those that are more typical of a structure of the complex ejecta type.

At WIND MC1 has a very short (9 hour) duration. It starts at hour 6 of 15 July (Day of year = 197) and ends on hour 14, inclusive, of the same day. MC2 occurs during the interval from hour 19 of 15 July to hour 9 of 16 July 2000. For both clouds neither start- nor end-time is certain to better than about 0.5 hour. The choice of boundaries is based, in both cases, on all of the relevant field and plasma observations, plus the trial and error attempts at model fitting as a check of choices. The specific characteristics used in these choices were: observations of the relatively smooth sweep of the field's latitude and longitude over the cloud from min to max for the latitude, the end of the sheath-like fluctuations for the cloud's front, the region of relatively smooth solar wind speed decrease which indicates that the cloud was expanding as it passed the WIND spacecraft, and other (quantitative) considerations to be described below where the cloud model is discussed. Figure 1 shows the upstream interplanetary shock (S2) at 14:35 UT on 15 July and a highly variable sheath between it and the front boundary of the cloud MC2. Within MC2 the proton density is irregular, as is common in magnetic clouds, but is not part of the standard definition of a magnetic cloud (Burlaga *et al.*, 1981; Burlaga, 1995). It

does not show any marked or special characteristics, except perhaps the rather low values in the latter 1/3 of the cloud's extent. The proton thermal speed is generally low and proton plasma beta is exceeding low over the full extent of both magnetic clouds. The proton thermal speed is significantly enhanced in the sheath behind S2 to values over 200 km s^{-1}, as might be expected for this exceedingly strong fast shock. Figure 1 shows that the speed drops across both clouds, gently for MC1 but very markedly for MC2. Changes of field longitude (ϕ_B) of about 180° are seen at revealing times throughout days 14, 15, and 16 July indicating the obvious presence of the heliographic current sheet (HCS), a not uncommon occurrence around ejecta/magnetic clouds (Klein and Burlaga, 1982). In fact, magnetic clouds have been seen to replace the HCS; such an event has been referred to as a HCS occlusion (Crooker and Intriligator, 1997; Crooker, Gosling, and Kahler, 1998). What we see in Figure 1 (large ϕ_B changes) is reminiscent of this. Notice that ϕ_B goes from 2nd quadrant values before MC2, especially noticeable early in the sheath, to 4th quadrant values just after the cloud, late on 16 July. This sheath region separates the two major events, i.e., the early ejecta/MC1 (mainly on 15 July) and later magnetic cloud MC2. Even before the earlier shock, S1, and immediately behind it, in its sheath, there are many large ϕ_B changes, of about 180°. All of this suggests the presence of the HCS around and between these ejecta. Most important is that ϕ_B is in the 4th quadrant for MC1 and in the 1st quadrant for MC2 after many switches in the sheath in front of MC2. Probably related to this (via the solar source) is that MC1 and MC2 θ_B-profiles are the mirror image of each other. This suggests that the two clouds will have the same field handedness, which is confirmed by our modeling. We now (1) establish a link between a halo-CME and MC2's plasma-field complex, (2) analyze both magnetic clouds' physical and geometrical characteristics, (3) estimate the interplanetary shock S2's normal and speed, and (4) examine some aspects of the solar wind-magnetosphere coupling.

2. Sun-to-Magnetic Cloud Transit Time

SOHO/LASCO and EIT (see descriptions by Brueckner *et al.*, 1995 and Delaboudinière *et al.*, 1995, respectively) observed a full halo-CME on 14 July 2000 (see, e.g., Webb *et al.*, 2000; St. Cyr *et al.*, 2000, and references therein). The event was first visible in C2 at 10:54 UT, as a bright front extending all around the occulting disk. The measured speed of the CME (averaged through 4 points in both the C2 and the C3 field before saturation from particles) was 1800 km s^{-1} at PA 262 (SW limb). This speed may suffer inaccuracies due to limitations of the high level of the proton event in LASCO's view. EIT observed a flare from AR9077 with a Moreton-like wave at 10:12 UT near disk center at location [N 16.8°; E 0.21°]. GOES satellites and solar observatories (*Solar Geophysical Data*) report an X5.7 3B class flare from this same area starting at 10:24 UT on 14 July. Because of

the closeness in time ($\Delta t \approx 40$ min) to the halo-CME, this flare was probably associated with it.

Since the magnetic cloud at WIND occurred over the 15-hour interval starting at hour 19 of 15 July (to 1.0 hour resolution), the center time of the cloud was at hour 03 of 16 July. Hence, the transit time from the time of the flare (at 10:24 UT on 14 July) to the cloud's mid-point was 41 ($\pm$ 0.5) hours which gives a transit speed of 1010 ± 20 km s^{-1} (where we use 1 AU $= 1.49 \times 10^8$ km). This agrees very well with the central speed of the magnetic cloud (≈ 1000 km s^{-1}) and with the average speed (990 km s^{-1}) used in the cloud modeling below; see Table II.

Likewise, observations of WIND/LEMT energetic ions (e.g., Reames, Ng, and Tylka, 2001) are assumed to provide an estimate of the start time of the CME which was 14 July 2000 11 UT, within about 30 to 60 min uncertainty. See Figure 1 (top) which shows the step flux increase of the 1-hour average MeV energetic ions (energetic channels which are 7.4–9.64 He^4 amu^{-1}, 9.20–13.4 O amu^{-1}, and 9.3–12.5 Fe amu^{-1}), marking the likely beginning of the shock driven by the fast ejecta that produced the halo-CME within a delay of approximately 1 hour. A second threshold-like sharp increase in each flux channel, between 15 and 16 UT on 14 July, marks the passage of S1. It is possible that two mechanisms further enhance these MeV energetic ions between the two shocks: (a) a better connection to the source after S1, and (b) 1st type Fermi acceleration between a slower (S1) and a faster (S2) shock. The 1st sharp decrease in these energetic particles occurs between 13 and 14 UT on 15 July marking the passage of the 2nd shock, S2, driven by the interplanetary magnetic cloud. A second step-decrease at 19 UT marks the entry of WIND into cloud MC2. Observations of kilometric type II radiation by WIND enables tracking of the ejecta/shocks from Sun to 1 AU (Reiner *et al.*, 2001), further supporting the link between MC2 at WIND and the halo-CME at the Sun on 14 July 2000.

3. Magnetic Cloud Analysis

Analyses of the clouds' magnetic structures are carried out using a force-free flux rope model (Lepping, Jones, and Burlaga, 1990; also see Burlaga, 1988) that we have used successfully often before for model-fitting magnetic clouds at 1 AU, and elsewhere, when the proton plasma beta was very low throughout the extent of the cloud. Most magnetic clouds at 1 AU have been shown to satisfy the force-free approximation (Goldstein, 1983; Marubashi, 1986; Burlaga, 1995). MC2 had the classic characteristics of a flux rope (observationally revealing a smoothly varying field direction) of low proton temperature, and strong field intensity, in this case an exceedingly strong intensity reaching values early in the cloud of over 60 nT. MC1 is also likely a magnetic cloud, but, as we will see, it is less certain and it is less well fit by the constant alpha flux rope model. The top part of Table II gives some 'observational quantities' associated with the two clouds, such as estimated

TABLE II
Magnetic cloud observational and model fit-parameters.

Parameter	Value, MC1	Value, MC2
Observations:		
Start time	DOY 197*, 06 hour	DOY 197, 19 hour
End time	DOY 197*, 14 hour	DOY 198, 09 hour
Duration (inclusive of end points)	9 hours	15 hours
Average speed of cloud	650 km s^{-1}	990 km s^{-1}
Average field intensity across the cloud	8.6 nT	41.7 nT
Model parameters:		
B_0 (axial field magnitude)	15.2 nT	46.8 nT
H (handedness of the field twist)	-1 (left-handed)	-1 (left-handed)
R_0 (radius of the cloud)	0.082 AU	0.189 AU
ϕ_A (longitude of cloud axis, GSE)	211°	46°
θ_A (latitude of cloud axis, GSE)	$-58°$	55°
$\mathbf{n}_A = (nx, ny, nz)$ (unit vector of axis in GSE)	$(-0.455, -0.272, -0.848)$	(0.394, 0.411, 0.822)
t_0 (center time from start of cloud)	3.5 hours	10.0 hours
$\lvert Y_0/R_0\rvert$ (relative impact parameter)	0.743	0.159
$\chi_R^2/(3N-n)$	0.0337	0.0169
asymmetry factor	0.211	0.333
Φ_0 (axial magnetic flux)	3.1×10^{20} Mx	52×10^{20} Mx

*DOY 197 is 15 July 2000.

start and end times, duration (on a 1-hour resolution basis), the average speed of protons within the cloud and average magnetic field intensity.

We start by discussing the model and applying it to MC2. Later we repeat the analysis for MC1. We assume that a magnetic cloud can be approximated locally by a static, constant-alpha, force-free, cylindrically-symmetric magnetic field configuration (Burlaga, 1988), given by the Lundquist (1950) solution of $\nabla^2\mathbf{B} = -\alpha^2\mathbf{B}$, which results from assuming $\mathbf{J} = \alpha\mathbf{B}$ and the use of Maxwell's equations. Other cloud models have considered the possibility that magnetic clouds expand as they move away from the Sun (Burlaga *et al.*, 1981; Farrugia *et al.*, 1992; Osherovich and Burlaga, 1997). We fit the Lundquist (1950) solution of $\nabla^2\mathbf{B} = -\alpha^2\mathbf{B}$ using the method of Lepping *et al.* (1990). The Lundquist (Bessel function) solution is

$$B_A(\text{axial}) = B_0 J_0(\alpha r), \quad B_T(\text{azimuthal}) = B_0 H J_1(\alpha r), \quad \text{and} \quad B_R(\text{radial}) = 0 \tag{1}$$

in cylindrical coordinates, where B_0 represents the axial field value and H (± 1) is the field handedness. A least-squares fit of these functions is initially made to unit normalized magnetic field data. Hence, only the field's direction is considered

at first. (A simple linear scaling of the model field's magnitude to the observed field's magnitude is done later to obtain B_0.) A 'reduced' chi-squared to the fit, $\chi_R^2/(3N - n)$, where N is the number of hour-average points and $n = 5$ is the number of parameters in this part of the fit, is used, among other parameters considering symmetry, to measure the 'quality' of the fit; the chi-squared quantity parameter is dimensionless. The full set of 7 fitted parameters are: B_0, the axial field intensity; H, the handedness of the field twist; R_0, the radius of the cloud; ϕ_A, A, the longitude and latitude of the cloud's axis (GSE coordinates), respectively; t_0, the center time; and Y_0, the closest approach (CA) distance from the axis; actually Y_0/R_0 (often called the relative impact parameter) is most generally used. The last 5 parameters (i.e., excluding B_0 and H) are the $n = 5$ considered in the reduced chi-squared fit process. We choose the boundaries of the cloud such that the magnetic field becomes purely azimuthal there; it is usually where $\alpha r = 2.4$ (then $r = R_0$).

The exact end-points are not always evident in magnetic cloud observations, and sometimes many trial-fits are necessary which was the case for both of these clouds. Choices of boundaries in these cases were based on a combination of the consideration of the characteristics of the plasma properties mentioned in the Introduction and on the results of this modeling. Specifically, these criteria were: (1) the minimization of $\chi_R^2/(3N - n)$, (2) maintaining low proton thermal speed throughout, and (3) a fairly good fit to the times when the bulk speed went from max to min (while ignoring the highest values just after the upstream shock (S2) in the case of MC2) and disallowing strongly asymmetric results. Asymmetry is measured by the asymmetry factor (a.s.f.), which is defined as $|(1-2t_0/N)|$, where N is the number of hours across the magnetic cloud, i.e., its time-of-passage in hours; a.s.f. = 0.0 is the desirable perfect symmetry (consistent with the model) and 0.5 or greater is quite poor. Table II provides the results of the model fit to the measured field; MC2's results are on the right side.

MC2's axis had an estimated longitude of $\phi_A = 46°$ and a latitude of $\theta_A = 55°$. High latitude cloud axes are not uncommon (see, e.g., Bothmer and Schwenn, 1998; Burlaga, 1988). MC2 had a strong central field of $B_0 = 46.8$ nT and a large radius of $R_0 = 0.189$ AU. Typical WIND B_0 and R_0 values (based on 34 events) are 16.4 ($\pm$ 4.4) nT and 0.14 ($\pm$ 0.05) AU, respectively (Lepping and Berdichevsky, 2000). The cloud had a left-handed helical field. We also see that the relative closest approach distance (impact parameter) was 0.16, indicating that the spacecraft came relatively close to the cloud's axis, i.e., only 16% of R_0 away. Figure 2 shows graphically the MC2's model results (solid-curve) plotted over the 1-hour average observations of the field in GSE coordinates, in terms of field magnitude $|\mathbf{B}|$ and angle representation. We notice that the direction of the observed field (given by the dotted curves of ϕ_B, θ_B) is well approximated by the model, especially the latitude of the field. This is expressed by the relatively good value of $\chi_R^2/(3N - n) = \chi_R^2/40 = 0.017$ (for $N = 15$ and $n = 5$), as Table II shows. The static model cannot describe expansion of a cloud (Farrugia *et al.*, 1992; Osherovich, Farrugia, and Burlaga, 1993; Osherovich and Burlaga, 1997), and therefore it is usually not very

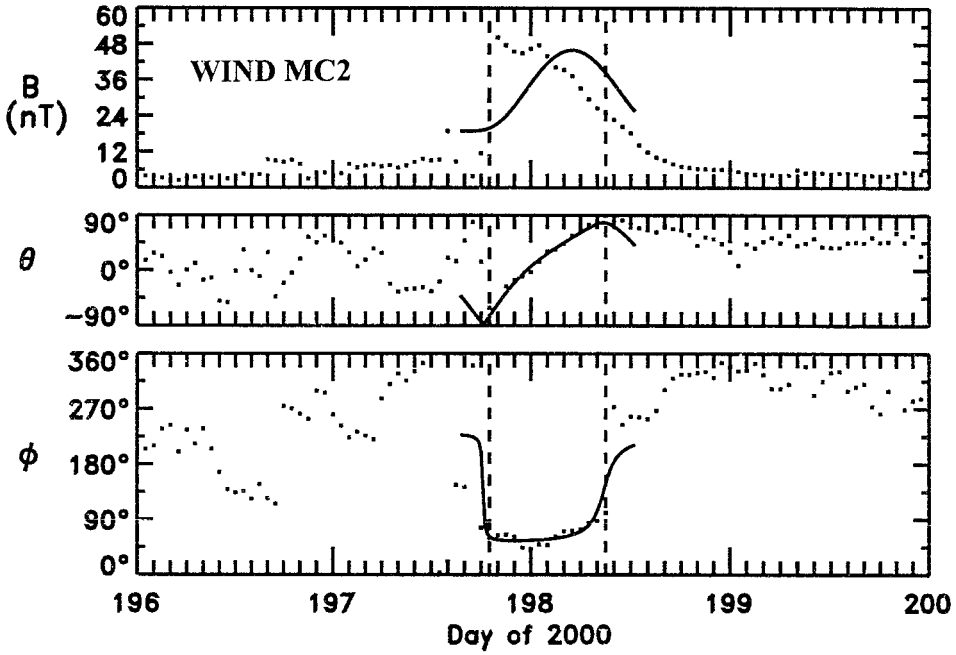

Figure 2. The results of the magnetic cloud model fit (*solid line curve*) for MC2 based on 1-hour averaged field data, shown by the *dotted curve*. The three panels are (*from top to bottom*) the field magnitude $|\mathbf{B}|$ and field latitude θ and longitude ϕ all in GSE coordinates.

good at fitting $|\mathbf{B}|$, as is the case here. As Figure 2 shows, the $|\mathbf{B}|$-fit is the poorest parameter fit, especially for the early part of the cloud. This is consistent with the intermediate-to-poor asymmetry factor of 0.33, indicating a not very symmetric field profile.

Using this same cloud model (Lepping, Jones, and Burlaga, 1990) we can estimate the magnetic flux (Φ_0) of a cloud (where $\mathbf{B}_A$ is the axial component of the field; see Equation (1)):

$$\Phi_0 = \int \mathbf{B} \cdot \mathbf{dS} = \int \mathbf{B}_A \cdot \mathrm{d}\mathbf{S} = B_0 \int J_0(\alpha r) 2\pi r \, \mathrm{d}r = 2\pi / B_0 \alpha^2 J_0(x) \, \mathrm{d}x \quad (2)$$

over x: 0–2.4, where $x \equiv \alpha r$ and $x_0 = \alpha R_0 = 2.4$, at the magnetic cloud's boundary according to the model. Hence,

$$\Phi_0 = 1.36 B_0 R_0^2. \quad (3)$$

Along with the fundamental fit parameters, Table I also provides the value of Φ_0. Because of the large size and exceedingly strong field of MC2, the flux (estimated to be about 52×10^{20} Mx) was the strongest yet seen for any WIND magnetic cloud. It is about five times the average axial flux seen for the WIND data set (average $= 10.4 \times 10^{20}$ Mx) (Lepping and Berdichevsky, 2000).

We now consider MC1, which is of relatively short duration, only 9 hours. The average duration of earlier WIND clouds is about 27 hours, but MC1 was passing WIND at a high speed of 650 km s^{-1}, and most earlier WIND clouds were moving at 400 km s^{-1} on average (Lepping and Berdichevsky, 2000). MC1 is assumed to be a magnetic cloud, because it appears to adequately satisfy (barely) the definition of a magnetic cloud, but the variation of field direction is not as smooth as is commonly seen in clouds, and its field intensity is unusually flat. Neither of these disqualifies it as a cloud, however. Its short duration is not a serious problem, because (as we will see) the spacecraft did not pass directly through its center and the cloud was traveling fast, as mentioned. The decrease in speed across it is, indeed, quite common and indicates an expanding structure. Most magnetic clouds are expanding at 1 AU. MC1's field intensity is elevated above normal values (of about 5.5 nT), but at about 10 nT it is considerably weaker than what is usually seen for clouds at 1 AU (18 nT). Also it is clear from Figure 1 that its proton temperature is sufficiently low to qualify. A supporting piece of evidence that MC1 is a unique field structure is the subtle but noticeable changes in the LEMT energetic particle fluxes at its assumed boundaries, as Figure 1 also shows. (Even more marked particle flux changes are seen at MC2's boundaries, especially at the end-boundary, whose exact position was otherwise in some doubt, at least by an hour or so.) Henceforth, we will refer to MC1 as a magnetic cloud without qualification, and now describe the results of cloud model fitting of the field within it.

The axis of MC1 had an estimated longitude of $\phi_A = 211°$ and a latitude of $\theta_A = -58°$. See the column under MC1 in Table II. The cloud had an average strength central field ($B_0 = 15.2$ nT) and a relatively small radius ($R_0 = 0.082$ AU). It also had a left-handed helical field. The impact parameter was 0.74, indicating that the spacecraft was fairly far from the cloud's axis at closest approach, i.e., 74% of R_0 away. This contrasts to MC2's situation where the spacecraft passage was very close to the cloud's axis. Figure 3 shows graphically MC1's model results (solid-curve) plotted over the 1-hour average observations of the field in the same format as in Figure 2. We notice that the direction of the observed field (given by the dotted curves of ϕ_B, θ_B) is fairly well approximated by the model, especially the latitude of the field, as in MC2's case. The angle ϕ_B is not quite as well approximated by the model. The evaluation of the model fit is expressed by the intermediate value of $\chi_R^2/(3N - n) = \chi_R^2/22 = 0.034$ (for $N = 9$ and $n = 5$), as Table II shows. This relatively large value indicates a not very good fit putting in some doubt all of the fit parameters for this cloud. As mentioned above, there may have been some expansion of MC1, as appears to be indicated by the gradient of speed shown in Figure 1, but the consequence of expansion is not indicated in the field profile. In any case, the B-profile is not very well fit for MC1. The asymmetry factor was 0.21, indicating a fairly symmetric profile of the field (of $|\mathbf{B}|$ especially) and slightly better than it was for MC2 (0.33).

The magnetic flux was 3.1×10^{20} Mx, only slightly lower than average. It is noteworthy that the cloud-axes $\mathbf{n}_A(1)$ and $\mathbf{n}_A(2)$ are 171° from each other which

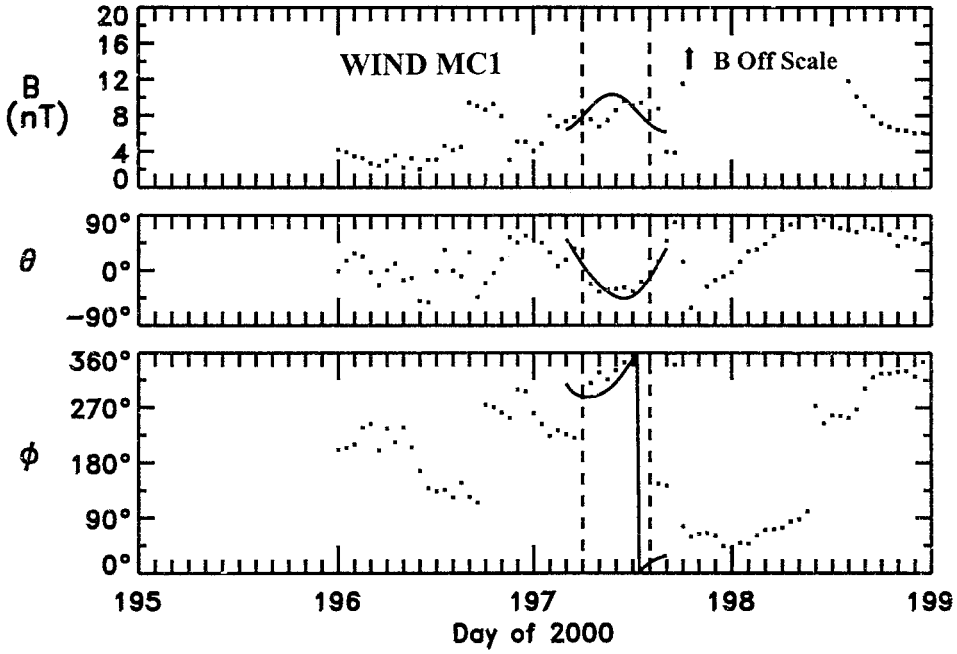

Figure 3. The results of the magnetic cloud model fit (*solid line curve*) for MC1 in the same format as that of Figure 2.

indicates that they were almost anti-parallel at the time of observation, but there is an error of about 20° on this determination. The reason for this relationship is not clear, but it could be associated with axial polarity splitting according to the flux-ropes' birthplace (initial) conditions in the vicinity of where the HCS is anchored to the Sun.

Both clouds had left-handed helical fields. But the magnetic flux of MC2 was about 17 times greater than that of MC1, due mainly to the considerable difference in cross-sectional sizes but also to the unusually strong fields of MC2. As mentioned in the Introduction, between the two clouds, especially in the sheath following S2, there appear to be many indications of HCS crossings. There are such indications all throughout the 3-day period of interest. A preliminary variance analysis of the magnetic field across the entire sheath region indicates a minimum variance direction that is about 18° (with a poor eigenvalue determination) from being perpendicular to MC2's axis. Some other carefully chosen large directional discontinuities within the sheath region also indicate this perpendicularity. Hence, the average plane of principal field variation of the field is apparently consistent with what would be expected for MC2's front boundary, if the HCS were directly influenced by that boundary.

TABLE III

Positions in GSE coordinates and UT times used in estimating the normal and speed upstream of MC2 from spacecraft in the solar wind.

Position	R_x (km)	R_y (km)	R_z (km)	Time on 15 July (UT)
ACE-MAG	1 575 600	120 360	99 562	14:16:35
WIND-MFI	1203	−440 150	−41 383	14:34:50
IMP-8 PLA	72 027	203 442	32 678	14:30–14:38
GEOTAIL-CPI	159 722	42 914	−10 538	14:35

4. Upstream Shock Analysis

Let us describe the shock (S2) upstream of MC2 and estimated its unit surface normal ($\mathbf{n}_S$) and speed (V_S). (S1 is discussed briefly below). First, we point out that S2 is a very strong shock whose ratio of downstream-to-upstream densities is very close to 4.0 ($\approx$ 33/8.2), as indicated in the (high resolution) data of Figure 4. The downstream-to-upstream ratio of magnetic field intensities is $\approx 2.3 \pm 0.3$, as seen in the figure. Since these ratios are distinctly unequal, this suggests a probable quasi-parallel nature for S2 (Burlaga, 1995). The quantities $\mathbf{n}_S$ and V_S are estimated below by using a combination of constraints that encompass the following: velocity coplanarity, magnetic field coplanarity, consistency of upstream field direction with the shock profile (e.g., a pulsation or 'parallel' shock must have an upstream IMF aligned with the shock-surface normal within about 30° (see Acuña *et al.*, 1981 and Burlaga, 1995)). Then we check for consistency among $\mathbf{n}_S$, V_S, observation-position and S2 encounter-time for the various spacecraft that were in the solar wind during the shock-cloud passage. (This is important, because of the approximate nature of the constraints being employed.) These spacecraft are WIND, GEOTAIL, ACE, and IMP-8. Table III lists the spacecraft positions and times at shock ramp passage for these various spacecraft.

The key constraints are the following:

(1) The observation that $\Delta\mathbf{V}_Y \approx \Delta\mathbf{V}_Z$ from the observed change in solar wind velocity from upstream (subscript 1) to downstream (2) (where $\Delta\mathbf{V} = \mathbf{V}_2 - \mathbf{V}_1$) seen in both IMP-8 and GEOTAIL data.

(2) Within the measured time resolutions (1 minute at GEOTAIL and 3 s at WIND) the shock passes WIND and GEOTAIL at almost the same time.

The resulting normal and speed are

$\mathbf{n}_S = (-0.93, +0.26, +0.26)$(with an error cone angle of about 5°) and

$V_S = 550 \pm 50$ km s^{-1},

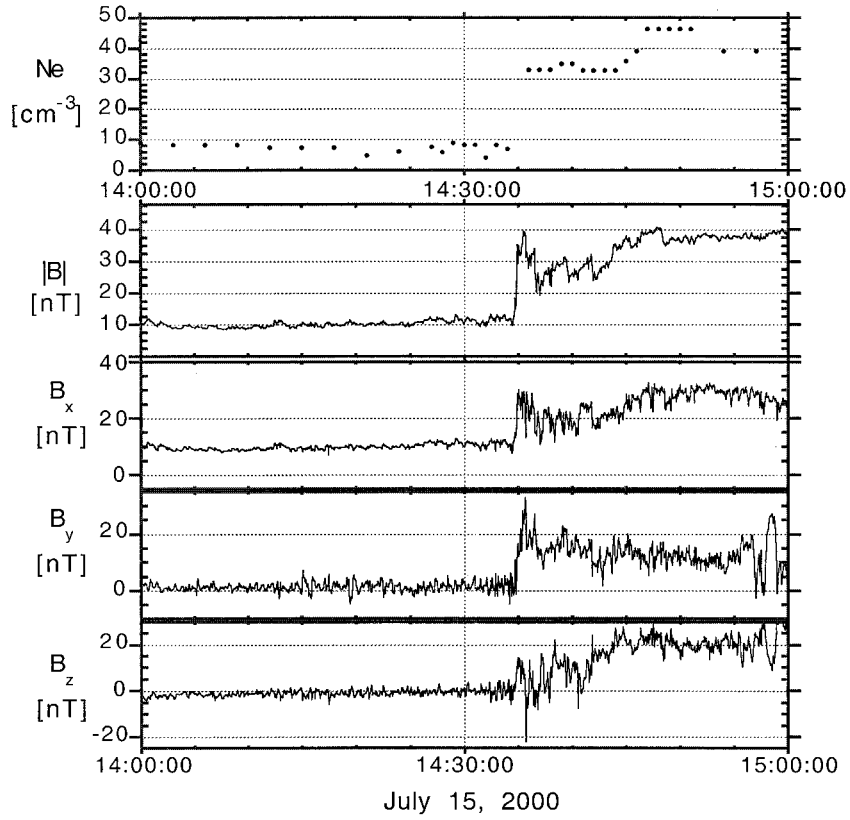

Figure 4. Detailed region of WIND data around the shock (S2) upstream of MC2 . The *top panel* is electron density from SWE data with WAVES derived densities added to the plot around the ramp to increase sample frequence. The *bottom four panels* give 3-s averages of the magnetic field in terms of magnitude |B| and Cartesian components, $B_{X,Y,Z}$ (GSE). The broad ramp and high degree of field fluctuations revealed in this case are characteristic of a 'pulsation' shock whose normal is usually aligned with the upstream field within 30°, a parallel shock being an extreme case. Time in UT.

where V_S is measured along $\mathbf{n}_S$ in the upstream solar wind plasma frame of reference. The upstream solar wind speed from IMP-8 and WIND along the normal is $V_{\rm UP} = 650 \pm 50$ km s^{-1}. The shock's magnetosonic Mach number is 6.5 ± 1.0 and its Alfvén Mach number is 7.5 ± 1.0. The techniques used here to determine uncertainties in $\mathbf{n}_S$ and V_S are described in Berdichevsky *et al.* (2000).

The angle between $\mathbf{n}_S$ and $\langle \mathbf{B}_{\rm UP} \rangle$ at WIND is ~ 20–$27°$ where $\langle \mathbf{B}_{\rm UP} \rangle$ is an average of the magnetic field over a region just in front of the shock. This relatively small angle is, therefore, consistent with what is required by a quasi-parallel shock. A similar principle concerning the *change in velocity* across the shock can be applied as a test of $\mathbf{n}_S$. That is, the angle between $\Delta\mathbf{V}$ and $\mathbf{n}_S$ must be small and is zero for a perfectly parallel shock (e.g., see Smith and Burton, 1988). We test this

using GEOTAIL's velocity data. Since $\Delta\mathbf{V}$(GEOTAIL) = (−300, 110, 110) km s^{-1}, the angle between $\mathbf{n}_S$ and $\Delta\mathbf{V}$ is $\approx 6°$, which is reasonably small, as expected.

We point out that this upstream shock (S2) normal $\mathbf{n}_S$ is perpendicular to MC2's axis ($\mathbf{n}_A$) to within about 2°, as might be expected if the cloud was driving the shock at or near the time of observation. We stress that $\mathbf{n}_S$ is relatively far off the Sun–Earth line (i.e., 26°) providing further support for our hypothesis that S2 is a driven shock at 1 AU, since driven shocks are more likely to be nonradial; a shock having strictly a solar source is expected to be nearly aligned with the Sun–Earth direction.

A different approach (i.e., one with an emphasis on different constraints) was employed to estimate S2's normal and shock speed (T. Terasawa, private communication). It employs information on the location and transit time of the upstream shock for many spacecraft along with considerations of field variance analysis. These techniques and the one used here give normals that are in agreement within 13° *in the limit of planar shock surface geometry*.

S1 is also a strong shock, and therefore must also require a driver to maintain its energy. The solar ejecta immediately following it must have been its driver. MC1 was at the downstream portion of that ejecta and is apparently not directly driving the shock. This hypothesis is consistent with the unusually long interval between S1 and the front of MC1, $\approx$ 14.5 hours (see Table I); this exceeds a realistic sheath duration at 1 AU. We also point out the fact that the speed of the ejecta immediately downstream of S1 is markedly faster than that of MC1. This could not be the case if MC1 were directly driving S1.

5. Input Energy and Momentum to Magnetosphere

The Bastille interplanetary events had major impact on the Earth's magnetosphere. For example, a complex multi-phase magnetic storm and severe magnetopause positional changes occurred. We examine here WIND interplanetary parameters that are known to control the transfer of energy and momentum to the magnetosphere that cause such dynamic effects. For the days 14–16 July (DOYS 196 through 198) Figure 5 shows interplanetary magnetic field intensity, IMF B_Z(GSM), solar wind ram pressure, estimated stagnation point distance (R_{MP}), B_Z(GSM)-component of the magnetic field from one of the favorably positioned GOES satellites (here called B_Z(GEO)), ε (Akasofu, 1981), induced electric field VB_S, and the geomagnetic storm index Dst. We point out that alternative formulae to VB_S and ε have been developed for estimating solar wind energy input to the magnetosphere (e.g., see Bargatze, McPherron, and Baker, 1986). Vertical lines in Figure 5 indicate where the two magnetic clouds (dashed) and their upstream shocks (solid) are located. The quantity R_{MP} (solid curve) is estimated from a static, pressure balanced, magnetopause model in which the external field is ignored (Choe, Beard, and Sullivan, 1973). However, during parts of this 3-day interval the external field was unusually strong, the magnetopause was very dynamic, and magnetic merging

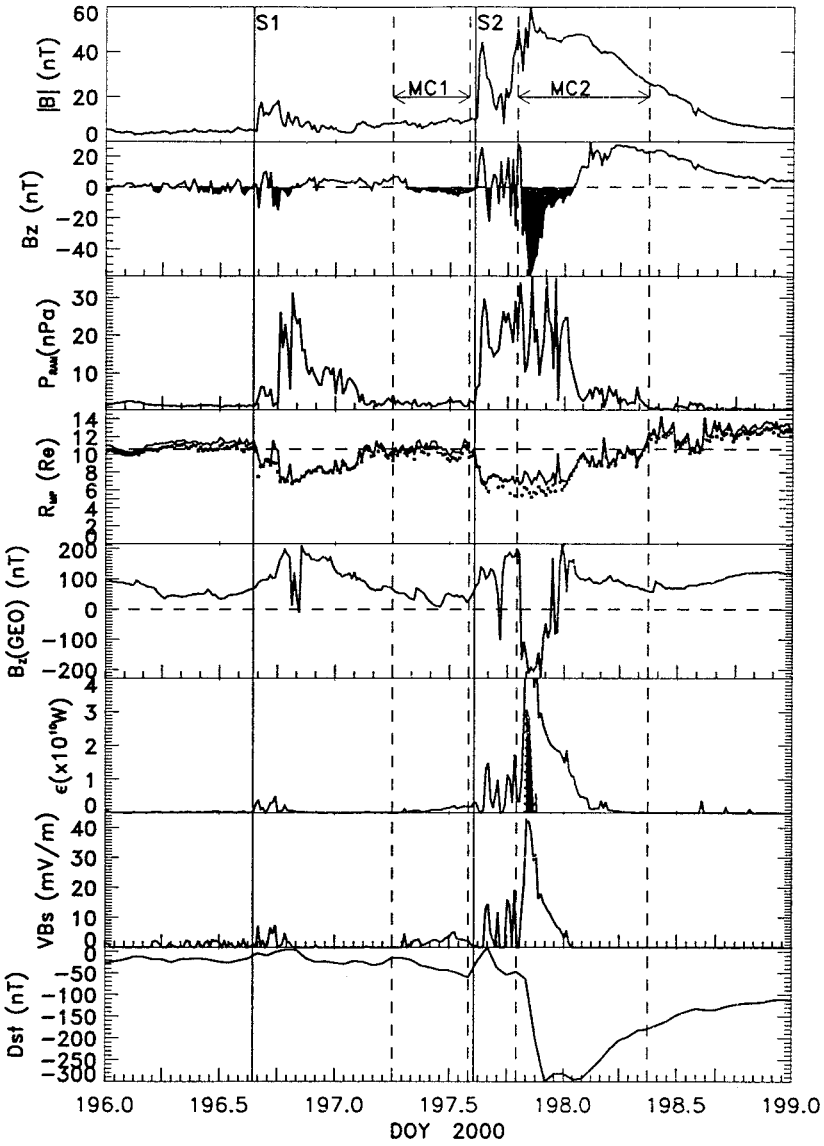

Figure 5. Comparisons of various quantities associated with the solar wind–magnetosphere interaction. These are (*from top to bottom*): interplanetary magnetic field magnitude (|**B**|), north-south component of the IMF (B_Z), solar wind ram pressure (P_{RAM}), estimated stagnation point standoff distance [R_{MP}, from Choe, Beard, and Sullivan, 1973 (*solid curve*), and from Shue *et al.*, 1997 (*dotted curve*)], B_Z component of the magnetic field from geosynchronous satellite GOES [called B_Z(GEO)], Akasofu (1981) ε, induced electric field (VB_Z), and the geomagnetic storm index *Dst*, for the three days of interest. (All are in 15 min average form, except *Dst*, and computations were done in GSM coordinates.) In panel 2, when B_Z is negative the region between the curve and the zero line is shaded.

sometimes occurred at the magnetopause (for B_Z-south), which must erode away some of the internal field and its pressure. Hence, we present the profile of R_{MP} (solid curve) only as an approximation of the actual position of the front-side boundary acknowledging that it will not be very accurate during very negative IMF B_Z or rapid solar wind momentum changes. Also owing to measurement limitations of some quantities over some intervals of Figure 5, this estimate of R_{MP} is considered to be an *upper* bound. To rectify part of this problem we add to the R_{MP} panel of Figure 5 another estimate (dotted curve), which accounts for the effects of large negative B_Z (Shue *et al.*, 1997). As expected, the dotted-curve is often lower than the solid-curve. R_{MP} varies considerably over the three days but is unusually small over most of the interval (with the exception of the region around MC1), because of the very fast solar wind. It reaches a minimum of about 5 R_E (dotted-line) at 20:48 UT on DOY 197, very early in MC2, and a maximum of about 16 R_E late in the cloud and just beyond, as the speed drops to pre-event conditions and where the density is low. In the R_{MP} panel a horizontal dashed-line is drawn at 10.6 R_E showing, for comparison, where the nominal 'magnetosheath' stagnation point distance is located. Geosynchronous orbit data from the GOES satellite support the dramatic changes estimated for R_{MP}. See the B_Z(GEO)-panel of Figure 5. The northern B_Z(GEO) excursions indicate strong magnetospheric compression sometimes to the point where the satellite GOES leaves the magnetosphere and finds itself in the sheath where the B_Z field tracks the IMF, going negative on four separate occasions, one being ≈ 5 hours long (early in MC2).

The panels in Figure 5 showing ε and VB_S indicate the unusually large power and induced electric fields (respectively) imparted to the magnetosphere after the time of S2 and especially during MC2. Figure 5 shows that *Dst* reaches a minimum of -300 nT shortly after entering MC2, i.e., during hour 22 of Day 197 (15 July). The complex nature of *Dst* is the direct reflection of the multiple (and long-lasting) regions of southward IMF B_Z, denoted by the shaded regions in the B_Z panel (GSM) in Figure 5. The latter portion of MC1 was responsible for a decrease in *Dst* to -60 nT (a modest storm) appearing quite small compared to the minimum *Dst* in response to the early region of MC2. In connection with MC2's upstream shock S2, an SSC occurred at hour 16 of 15 July (just before the minimum in R_{MP} (dotted curve)), as the local peak in the *Dst* curve shows, and shortly after S2, as expected.

6. Summary and Conclusions

The interplanetary characteristics of the Bastille Day events observed near Earth occurring over the days 14–16 July 2000 have been described and analyzed. Table I outlines the main features in the sequence of events in this complex, and Figure 1 shows a physical overview. We see that two interplanetary shocks (S1 and S2) occurred during this time and probably two magnetic clouds, the second one (MC2)

having very impressive characteristics. The profiles of the 10-MeV (WIND/LEMT) energetic ions (He^4, O, and Fe) in Figure 1 (top) give an indication of the solar source initiation-time, particle trapping between the two interplanetary shocks, and more subtle changes delineating the boundaries of the two magnetic clouds. Hence, these measurements help to organize the overall sequence of events from the solar source to 1 AU. A giant magnetic storm occurred (with min Dst lower than -300 nT) late on the 15th, along with major magnetospheric compression to magnetopause distances lower than geosynchronous orbit (6.6 R_E), due to the high intrinsic ram pressure resulting from the high speed of the solar wind and also to strong negative IMF B_Z values. This is especially dramatic at and around the front of MC2 for about 4 hours during which the solar wind speed was ≈ 1100 km s^{-1}, IMF $B_Z \approx -60$ nT, and R_{MP} was at least as low as 5 R_E. Such high speeds were not attained by any of the WIND clouds observed over the earlier, quieter, years, although other high ram pressures have been observed which were due to high densities in those cases; the densities were not unusually high in this complex, except perhaps around hour 0.0 of 15 July in a region of apparent solar ejecta separating S1 from MC1. The high ram pressure due jointly to high speed and relatively high density pushed in the front of the magnetosphere to geocentric distances as low as 6 R_E at that time. The estimated large excursions in R_{MP} were consistently supported by B_Z-observations from the GOES satellites in geosynchronous orbit, revealing magnetospheric field compression and on several occasions sheath fields.

A static force free field model was used to fit the WIND field profile of both clouds. This provided estimates of the clouds' various physical and geometrical characteristics, as given in Table II. The clouds had markedly different cross-sectional sizes (R_0 (1) = 0.082 AU and R_0 (2) = 0.189 AU). MC2 had a very strong axial field (46.8 nT) giving it, along with its very large cross-sectional size, the largest axial magnetic flux (52×10^{20} Mx) of any magnetic cloud observed at WIND since launch, being about a factor of 5 times the average flux during that 'quiet period', (i.e., over 3.8 years from 34 clouds) and 17 times the flux of MC1. Both clouds had left-handed magnetic helicity.

Both magnetic clouds had associated strong shocks, but MC1 was apparently not directly driving its upstream shock (S1). S2 occurred about 4.5 hours ($= \Delta t_{S2}$) upstream of MC2. An important finding was that S2's shock surface normal was perpendicular to the estimated MC2 cloud axis, within 3°, but was 22° from the Sun-Earth line. This, along with the small Δt_{S2} and large size of MC2, indicates that MC2 was very likely directly driving the shock, at least at the time of shock observation. It was an unusually fast shock having a speed of 550 ± 50 km s^{-1} (along the normal) relative to the upstream solar wind which gave a net shock speed along - X_{GSE} of 1075 km s^{-1}. The shock's speed was consistent with the cloud's front speed of about 1100 km s^{-1}; this correspondence is not unusual (see, e.g., Lepping *et al.*, 2001; Berdichevsky *et al.*, 2001). The shock's magnetosonic Mach number (with $T_e \sim 3.0 \times 10^5$ K) was 6.5 ± 1.0 and its Alfvén Mach number was 7.5 ± 1.0.

From the estimated longitudinal orientation of both magnetic clouds it is likely that Earth encountered the ejecta-cloud complex on its flank, well away from the clouds' 'nose' regions. This is well determined by the cloud model but can be seen directly from examination of ϕ_B of Figure 1 for both clouds; both longitudes were relatively far from the Y_{GSE}-axis. Also, it is likely that there were major interactions of the shocks-ejecta/clouds (and therefore intersections of these structures) at some heliographic longitudes between the Sun and 1 AU for these structures to have been observed in the temporal sequence that occurred near Earth. Interplanetary shocks are sometimes detected inside magnetic clouds (e.g., Collier *et al.*, 2001).

Acknowledgements

We thank K. Ogilvie, the PI of WIND/SWE plasma data for use of these data, L. Frank, PI of GEOTAIL/CPI for access to these high-resolution data, A. Szabo, F. Mariani, and T. Narock for calibration and handling of WIND/MFI data, and R. Fitzenreiter for preliminary estimates of the electron temperature with WIND/SWE. We are also indebted to W. Mish and the ISTP/Science Operation and Planning Facility and the CDHF for enabling access to multiple data sets, on which substantial parts of this study are based. Two of us (RPL and DBB) acknowledge support from NASA, grant number NAG5-10883.

References

Acuña, M. H., Burlaga, L. F, Lepping, R. P., and Ness, N. F: 1981, in H. Rosenbauer (ed.), *Solar Wind Four*, Rep. MPAE-100-81-31, Max Plank Institute, Lindau, Germany, p. 143.

Akasofu, S.-I.: 1981, *Space Sci. Rev.* **28**, 121.

Bargatze, L. F., McPherron, R. L., and Baker, D. N.: 1986, in Y. Kamide and J. A. Slavin (eds.), *Solar Wind-Magnetosphere Coupling*, Terra Scientific Publ. Co., Tokyo, pp. 101–109.

Berdichevsky, D. B. *et al.*: 2000, *J. Geophys. Res.* **105**, 27 289.

Berdichevsky, D. B. *et al.*: 2001, *Ann. Geophys.*, submitted.

Bothmer, V. and Schwenn, R. H.: 1998, *Ann. Geophys.* **16**, 1.

Brueckner, G. E. *et al.*: 1995, *Solar Phys.* **162**, 357.

Burlaga, L. F.: 1988, *J. Geophys. Res.* **93**, 7217.

Burlaga, L. F.: 1995, *Interplanetary Magnetohydrodynamics*, Oxford University Press, New York.

Burlaga, L. F., Sittler, E., Mariani, F., and Schwenn, R.: 1981, *J. Geophys. Res.* **86**, 6673.

Choe, J. T., Beard, D. B., and Sullivan, E. C.: 1973, *Planetary Space Sci.* **21**, 485.

Collier, M. R. *et al.*: 2001, *J. Geophys. Res.* **106**, 15985.

Crooker, N. U. and Intriligator, D. S.: 1997, *J. Geophys. Res.* **102**, 24 343.

Crooker, N. U., Gosling, J. T., and Kahler, S. W.: 1998, *J. Geophys. Res.* **103**, 301.

Delaboudinière, J.-P. *et al.*: 1995, *Solar Phys.* **162**, 291.

Farrugia, C. J. *et al.*: 1992, in R. Schwenn (ed.), *Solar Wind Seven*, Pergamon, New York, p. 61.

Goldstein, H.: 1983, M. Neugebauer (ed.), *Solar Wind Five*, NASA Conf. Publ., 2280, p. 731.

Gopalswamy, N. *et al.*: 1998, *Geophys Res. Lett.* **25**, 2485.

Gosling, J. T.: 1990: in C. T. Russell, E. R. Priest, and L. C. Lee (eds.), *Physics of Magnetic Flux Ropes*, *Geophys. Monogr. Ser.* **58**, AGU, Washington, DC, p. 343.

Klein, L. W. and Burlaga, L. F.: 1982, *J. Geophys. Res.* **87**, 613.
Lepping, R. P. and Berdichevsky, D. B.: 2000, *Recent Research Developments in Geophysical Research*, Issue 3, Research Signpost, Trivandrum-8, India, p. 77.
Lepping, R. P., Jones, J. A., and Burlaga, L. F.: 1990, *J. Geophys. Res.* **95**, 11 957.
Lepping, R. P. *et al.*: 1995, *Space Sci. Rev.* **71**, 207.
Lepping, R. P., Berdichevsky, D. B., Szabo, A., Lazarus, A. J., and Thompson, B. J.: 2001, *Adv. Space Res.* **26**, in press.
Lundquist, S.: 1950, *Arkiv Fys.* **2**, 361.
Marubashi, K.: 1986, *Adv. Space Res.* **6**, 335.
Mulligan, T., Russell, C. T., Anderson, B. J., and Acuña, M. H.: 2001, *Geophys. Res. Lett.*, submitted.
Ogilvie, K. W. *et al.*: 1995, *Space Sci. Rev.* **71**, 55.
Osherovich, V. I. and Burlaga, L. F.: 1997, in N. Crooker *et al.* (eds.), *Coronal Mass Ejections*, GM 99, Washington, D. C., AGU, p. 157.
Osherovich, V. I., Farrugia, C. J., and Burlaga, L. F.: 1993, *Adv. Space Res.* **13**, 57.
Reames, D. V., Ng, C. K., and Tylka, A. J.: 2001, *Astrophys. J.* **548**, L233.
Reiner, M. *et al.*: 2001, *Solar Phys.*, this issue.
Shue, J.-H. *et al.*: 1997, *J. Geophys. Res.* **102**, 9497.
Smith, E. J. and Burton, M. E.: 1988, *J. Geophys. Res.* **93**, 2730.
Smith, C. W. *et al.*: 2001, *Solar Phys.*, this issue.
St. Cyr, O. C. *et al.*: 2000, *J. Geophys. Res.* **105**, 18 169.
von Rosenvinge, T. T. *et al.*: 1995, *Space Sci. Rev.* **71**, 155.
Webb, D. F. *et al.*: 2000, *J. Geophys. Res.* **105**, 7491.